HHS Public Access

Author manuscript

Psychiatry Res. Author manuscript; available in PMC 2018 August 30.

Published in final edited form as:

Psychiatry Res. 2017 August 30; 266: 53–58. doi:10.1016/j.pscychresns.2017.06.003.

Computerized cognitive training for children with neurofibromatosis type 1: a pilot resting-state fMRI study

Yuliya N. Yoncheva[a], **Kristina K. Hardy**[b,c], **Daniel J. Lurie**[d], **Krishna Somandepalli**[e], **Lanbo Yang**[a], **Gilbert Vezina**[c,f], **Nadja Kadom**[g], **Roger J. Packer**[b,c], **Michael P. Milham**[h,i], **F. Xavier Castellanos**[a,i], and **Maria T. Acosta**[b,c,*]

[a]Department of Child and Adolescent Psychiatry, NYU Langone Medical Center, New York, NY, USA

[b]Department of Pediatrics and Neurology, George Washington University, School of Medicine, Washington, DC, USA

[c]Children's National Health System, Washington, DC, USA

[d]Department of Psychology, University of California, Berkeley, Berkeley, CA, USA

[e]School of Engineering, University of Southern California, Los Angeles, CA, USA

[f]Department of Diagnostic Imaging and Radiology, Children's National Health System, Washington, DC, USA

[g]Department of Radiology and Imaging Sciences, Children's Healthcare of Atlanta (Egleston), Atlanta, GA, USA

[h]Child Mind Institute, New York, NY, USA

[i]Nathan Kline Institute for Psychiatric Research, Orangeburg, NY, USA

Abstract

In this pilot study, we examined training effects of a computerized working memory program on resting state functional magnetic resonance imaging (fMRI) measures in children with neurofibromatosis type 1 (NF1). We contrasted pre- with post-training resting state fMRI and cognitive measures from 16 participants (nine males; 11.1±2.3 years) with NF1 and documented working memory difficulties. Using non-parametric permutation test inference, we found significant regionally specific differences (family-wise error corrected) in two of four voxel-wise resting state measures: fractional amplitude of low frequency fluctuations (indexing peak-to-trough intensity of spontaneous oscillations) and regional homogeneity (indexing local intrinsic

*Corresponding author: Maria T. Acosta, MD Associate Professor Clinical Director, The Gilbert Family Neurofibromatosis Institute Department of Pediatrics and Neurology George Washington University Children's National Health System 111 Michigan Av. NW Washington DC, 20010, USA Phone 202-476-5181. macosta@childrensnational.org.

Conflict of interest:
The authors declare that they have no conflict of interest.

synchrony). Some cognitive task improvement was observed as well. These preliminary findings suggest that regionally specific changes in resting state fMRI indices may be associated with treatment-related cognitive amelioration in NF1. Nevertheless, current results must be interpreted with caution pending independent controlled replication.

Keywords

NF1; BOLD; pediatric; brain training; working memory; regional homogeneity; fractional amplitude of low frequency fluctuations

1. Introduction

Although cognitive deficits in attention, working memory and executive function are among the most impairing consequences of neurofibromatosis type 1 (NF1) (Acosta et al., 2006; Schwetye and Gutmann, 2014), evidence-based, effective interventions that improve or restore cognitive function in NF1 remain lacking. Computerized cognitive training programs may augment cognitive abilities through repeated practice of mental exercises with increasing difficulty as performance improves (e.g., Klingberg et al., 2005). Cogmed [www.cogmed.com] is a computerized visuo-spatial training regimen administered at home and supplemented by remote coaching sessions (Astle et al., 2015; Holmes et al., 2009; Olesen et al., 2004). In developmental and acquired attentional disorders, Cogmed gains have been reported to be sustainable for months and to span across multiple cognitive measures, including certain untrained tasks (Astle et al., 2015; Conklin et al., 2015; Holmes et al., 2009; Stevens et al., 2016).

Consistent with training-induced neural plasticity (Kelly and Castellanos, 2014), Cogmed interventions may modulate blood-oxygenation level-dependent (BOLD) signals during tasks probing working memory and cognitive control (Olesen et al., 2004; Stevens et al., 2016). Such training effects tend to manifest as increased prefrontal activity as well as enhanced connectivity within prefrontal cortex, and between prefrontal and parietal regions (for review see, Constantinidis and Klingberg, 2016; Nee et al., 2013). For instance, in typically developing children, ages 8 to 11, Cogmed training has been found to induce intrinsic functional connectivity alterations between fronto-parietal and ventral visual areas (Astle et al., 2015).

While the neural correlates of NF1 are understudied, aberrant recruitment of visual and default mode network regions in response to checkerboards has been reported in children and in adults with NF1 (Violante et al., 2012). Preliminary evidence suggests that resting state (i.e., task-free) BOLD activity patterns in NF1 may be modifiable (e.g., by pharmacological treatment: Chabernaud et al., 2012). Relative to healthy controls, abnormal resting state functional connectivity has also been identified in NF1 (Loitfelder et al., 2015; Tomson et al., 2015).

This pilot open-label, prospective pre-/post-test study assessed training effects of Cogmed on resting state fMRI measures in 16 NF1 patients (aged 8–15 years) with marked working memory deficits. We sought to identify reliable regionally specifiable changes in

spontaneous BOLD fluctuations by contrasting pre- with post-treatment resting state scans. Accordingly, we performed univariate voxel-wise analyses on a set of four indices of spontaneous resting state activity that have been used previously to examine neural correlates of working memory in typically developing children and adolescents (Yang et al., 2015), including two regional measures – fractional amplitude of low frequency fluctuations (fALFF, Zou et al., 2008) and regional homogeneity (ReHo, Zang et al., 2004). Additionally, to probe behavioral improvement, standardized Cogstate tasks (Maruff et al., 2009) were administered before and after Cogmed training completion.

2. Methods

2.1. Participants

Children with NF1 (age range: 8–15 years) were identified through an institutional NF1 clinical database with approval of the Children's Health System Institutional Review Board. After obtaining written informed consent and assent, children's intellectual, working memory and executive function skills were assessed. Participation was limited to children who exhibited working memory difficulties, specifically (1) score ≥ 1 SD below the population mean on the Wechsler Intelligence Scale for Children-IV (Wechsler, 2004) Working Memory Index or (2) T-score ≥ 75th percentile on the Metacognition scale of the parent-reported Behavior Rating Inventory of Executive Function (Gioia et al., 2000). Exclusionary criteria included: Wechsler Abbreviated Scale of Intelligence (Wechsler, 1999) estimated full-scale IQ < 70; motor, visual or auditory handicaps preventing computer use; a DSM-IV Axis I diagnosis that would take treatment precedence over cognitive training needs; history of photosensitive seizures; change in type or dose of psychotropic medication within the last 30 days; and chemotherapy for a brain tumor.

Qualifying children underwent resting state fMRI scans and a cognitive test battery (i.e., Cogstate testing; see 2.3) before and after completing Cogmed training, which resulted in 20 complete datasets. The at-home standard Cogmed training under parental supervision lasted ~25 sessions over 6–10 consecutive weeks. Weekly coaching phone calls by study staff were intended to troubleshoot potential problems and reinforce compliance. Algorithmic adaptive adjustment of training item difficulty on a trial-by-trial basis was used to ensure that performance was continually challenged over the course of each 30–45 minute training session. While a blinded, placebo-controlled study would have allowed inferences about efficacy and specificity, the primary goal of this pilot study was to determine whether reliable neural changes could be detected after computerized cognitive training in individuals with NF1. Accordingly, like previous clinical trials in attentional disorders (e.g., Stevens et al., 2016), we pursued an open-label approach.

Next, neuroimaging data quality was assessed. Inclusion required anatomical scans that passed visual quality assurance for signal drop-out and motion artifacts and functional scans with acceptable head motion, i.e., mean frame-wise displacement (FD_{mean}) ≤ 0.5 mm (Power et al., 2014), as computed using Jenkinson's formula (Jenkinson et al., 2002). This criterion yielded 16 subjects (nine males, mean age: 11.1 ± 2.3 years, range: 8–15 years, see Table 1 for participant characteristics) with usable pre- and post-Cogmed data (maximal

FD_{mean} = 0.375 mm, average FD_{mean} = 0.198 mm), whose data form the basis of further analyses reported here.

2.2. Neuroimaging data

2.2.1. Data acquisition—We obtained T1-weighted anatomical images (sagittal 3D fast spoiled gradient echo sequence: TR = 7.8 ms; TE = 30 ms; TI = 450ms; flip angle = 12°; voxel-size = 0.923 mm × 0.923 mm × 1.0 mm) and functional T2*-weighted resting state scans (echo planar images: TR = 2500 ms; TE = 25 ms; flip angle = 90°; 38 slices; voxel-size = 3.75 mm × 3.75 mm × 3 mm; 150 time-points) using a GE 3 Tesla scanner equipped with an 8-channel head coil.

2.2.2. Data pre-processing—Pre-processing was carried out using the open-source, Nipype-based, automated Configurable Pipeline for the Analysis of Connectomes (C-PAC) v0.3.3 [https://github.com/FCP-INDI/C-PAC/tree/0.3.3_development]. After discarding the first 4 time-points of each functional run to allow magnetization to reach steady state, pre-processing individual resting state functional scans consisted of 3D motion correction (realignment using the Friston 24-parameter model (Friston et al., 1996): 3 translational and 3 rotational parameters, their values from the previous time-point, and the squared values of these 12 items), nuisance regression (detailed in 2.2.2.2), temporal band-pass filtering (0.01–0.1 Hz) except for fALFF computation, registration (detailed in 2.2.2.3), and spatial smoothing using a 4-mm Gaussian kernel at full-width half maximum. The human-readable C-PAC pipeline configuration file is available online as Supplementary Information (SI_CPACconfig.yml).

2.2.2.1. Head micro-motion: *Head micro-motion*, indexed by Jenkinson's FD_{mean}, did not differ significantly pre- vs. post-intervention (t_{15} = 0.24, p = 0.82; FD_{pre} = 0.201 ± 0.09 mm, FD_{post} = 0.196 ± 0.09 mm).

2.2.2.2. Nuisance regression: To control for head motion effects and attenuate irrelevant signals, we used a subject-level nuisance regression strategy involving application of CompCor (Behzadi et al., 2007) with 5 principal components derived from white matter and cerebrospinal fluid using subject-specific masks along with regressing out preprocessed data on the 24 Friston parameters (Friston et al., 1996) generated from the motion correction procedure. Global signal was not regressed out (Yan et al., 2013a, 2013b).

2.2.2.3. Image registration: To ensure robust image registration of both sets of longitudinal scans, we adopted an unbiased pairwise approach (Reuter et al., 2012). Using the Advanced Normalization Tools (ANTs) algorithm for every participant, pairwise registration was performed with the common "midway" points between the pre-and post-Cogmed anatomical scans. Following functional-to-anatomical image co-registration, images were transformed into MNI152 (Montreal Neurological Institute) space at 2 mm^3 isotropic resolution using ANTs.

2.2.3. Resting state measures—Following data pre-processing, four resting state measures were computed (Yang et al., 2015): amplitude of low frequency fluctuations

(ALFF; Zang et al., 2007); fractional amplitude of low frequency fluctuations (fALFF; Zou et al., 2008); regional homogeneity (ReHo; Zang et al., 2004), and voxel mirrored homotopic connectivity (VMHC; Zuo et al., 2010b).

For ALFF and fALFF, in subject's native space, voxel time-series were transformed into power spectrum representations. ALFF was calculated as the total power in the frequency range between 0.01 and 0.1 Hz, thereby indexing the intensity of low frequency oscillations (Zang et al., 2007). fALFF was computed as the power within the low frequency range (0.01–0.1 Hz) divided by the total power in the entire detectable frequency range, thus representing the relative contribution of specific low frequency oscillations to the full range (Zou et al., 2008; Zuo et al., 2010a). For both measures, power in subject-level maps was transformed into z-scores to generate standardized subject-level maps.

ReHo was calculated for each individual subject as the Kendall's Coefficient of Concordance (KCC) between the time-series of a given voxel and its 26 nearest neighbors (Zang et al., 2004). Values of KCC range from 0 to 1 with higher values indicating greater similarity between the time-series of a given voxel and the adjacent voxels. Subject-level KCC maps were z-score standardized to enable group analysis.

VMHC assumes symmetric morphology between the left and right hemispheres; therefore individual brains were first transformed to fit a symmetric template. Functional data were then transformed to fit the new symmetrical anatomical image. VMHC was computed as the Pearson's correlation coefficient between the time-series of a given voxel and its symmetrical inter-hemispheric counterpart (Zuo et al., 2010b).

These four resting state measures have been previously examined in typically developing children and adolescents (e.g., Yang et al., 2015) and highlight distinct properties of intrinsic brain signals. Specifically, ALFF and fALFF quantify the amplitude of the low frequency oscillations that are a fundamental feature of intrinsic brain activity. The relative magnitudes of such fluctuations can serve as markers of individual differences or dysfunction. Both ALFF and fALFF show high sensitivity to gray matter signals, although ALFF is more susceptible to physiological noise (Zou et al., 2008; Zuo et al., 2010a).

ReHo measures local synchronization and has been associated with individual differences in behavioral inhibition in healthy adults (Tian et al., 2012) or resting state alterations in brain networks implicated in attention-deficit/hyperactivity disorder (ADHD; Cao et al., 2006).

VMHC quantifies the strength of inter-hemispheric synchrony in patterns of spontaneous activity (its most robust feature) and can be sensitive to age-related differences (Zuo et al., 2010b).

2.2.4. Statistical inference—In light of recent empirical demonstrations that parametric statistical inference tends to inflate family-wise error rates (Eklund et al., 2016), we opted for group-level non-parametric, permutation-based statistical inference. To minimize problems inherent to cluster-based inference, e.g., spatial smoothing and cluster-forming threshold dependence, we adopted the threshold-free cluster enhancement (TFCE, Smith and Nichols, 2009) algorithm. Permutation testing (10,000 randomizations), which controls for

multiple comparisons with family-wise error rate at $\alpha = 0.05$, was implemented in *fsl* v5.0.8′s *randomise* tool (Winkler et al., 2014) [http://fsl.fmrib.ox.ac.uk/fsl/fslwiki/Randomise]. Due to its use of cluster-wise evidence at each voxel, TFCE can reliably detect small, focal effects that may be missed by other methods. The algorithm's sensitivity to a wide range of signal shapes further renders it particularly suitable for our data-driven examination spanning different resting state measures (ALFF, fALFF, ReHo, VMHC) each with its unique signal properties. Paired pre- vs. post-Cogmed t-tests included head motion (FD_{mean}) as a nuisance covariate. Whole-brain un-thresholded statistical maps for all four resting state measures are freely accessible as 3D interactive images online [http://neurovault.org/collections/ZLEIBWYV] to enable exploration of the magnitude and spatial extent of sub-threshold effects.

2.3. Cognitive measures

Six Cogstate tasks - Detection, Identification, One-back, One Card Learning, Continuous Paired Associate Learning and Groton Maze Learning (Maruff et al., 2009) -were administered prior to and following Cogmed training completion. The CogState standardized battery [http://cogstate.com/computerized-tests/cognitive-tests/battery] was chosen due to its high test-retest reliability and negligible practice effects in healthy individuals across different exam settings (Cromer et al., 2015; Falleti et al., 2006). Task performance (speed or accuracy as per Maruff et al., 2009) was contrasted pre- vs. post-training within subjects using paired t-tests. Test statistics and Hedges' gav corrected effect sizes for small, correlated samples (Lakens, 2013) for age-normed scores are reported in Table 2. P-value adjustment for false discovery rate at $\alpha = 0.05$ (Benjamini and Hochberg, 1995) was calculated using the *p.adjust* function in R version 3.0.2.

Age-normed values for the Continuous Paired Associate Learning task were not made available by Cogstate at the time of data collection. However, given the non-significant difference for the Continuous Paired Associate Learning task (pre-Cogmed accuracy = 80.8% ± 3.3 vs. post-Cogmed accuracy = 80.0% ± 3.5), the lack of normative scores has little impact. The central findings reported in Table 2 remained practically unchanged when analyses were replicated using raw scores for the six Cogstate tasks (Table S1).

3. Results

Whole-brain contrasts of pre- with post-intervention maps revealed significant ($p < 0.05$, family-wise error corrected) regional differences in two resting state measures: fALFF and ReHo (Table 3). Specifically, we found decreased fALFF following Cogmed treatment in three clusters: the largest cluster was predominantly in left cerebellum I-IV extending medially, the second largest was mostly in right cerebellum V, and the smallest cluster was bilateral thalamus (Figure 1). Reduced post-treatment ReHo was observed in right superior frontal sulcus while increased ReHo was detected in a visual region: left occipital fusiform gyrus. Whole-brain un-thresholded statistical maps for these fALFF and ReHo effects, as well as for ALFF and VMHC are freely viewable online at http://neurovault.org/collections/ZLEIBWYV.

After adjusting for false discovery rate at $\alpha = 0.05$, two Cogstate tasks showed significant post-intervention improvement: Identification task speed and Groton Maze Learning accuracy increased (Table 2; raw scores in Table S1).

4. Discussion

This pilot investigation revealed preliminary evidence of Cogmed training effects on neural measures and cognitive performance in a small sample of children with NF1. Intervention effects ($p < 0.05$, corrected) were found for two local resting state measures. Following training, ReHo increased in higher order visual areas. Enhanced local synchrony within visual cortex post-intervention can be considered in the context of decreased BOLD activation across visual areas reported in NF1 relative to healthy controls (Violante et al., 2012). Moreover, given emerging evidence that visual processing deficits in NF1 might be more closely linked to poor attentional allocation rather than sensory impairments (Ribeiro et al., 2014), we speculate that our short-term training could have promoted greater synchrony within visual cortex via top-down mechanisms (Astle et al., 2015; Constantinidis and Klingberg, 2016).

Decreased ReHo was observed in a frontal cluster that overlaps with frontal networks whose connectivity tends to exhibit sensitivity to working memory training (Constantinidis and Klingberg, 2016). In fact, our cluster falls within 5 mm of the right caudal superior frontal sulcus peak [34, 6, 56; MNI] identified as a hub for maintenance of visuo-spatial information in a meta-analysis delineating components of working memory (Nee et al., 2013). The frontal modulation we observe is also consistent with a recent ADHD intervention study illustrating Cogmed training effects in frontal areas near superior frontal sulcus (Stevens et al., 2016).

The normalized resting state measure we probed in the frequency domain, fALFF, yielded significant intervention effects in cerebellum and thalamus. Given the U-shaped age-related trajectory of fALFF patterns associated with working memory in healthy children and adolescents (Yang et al., 2015), the direction of the training effect in the current study might reflect developmental effects, although we cannot test this speculation in our pilot sample. The cerebellar and thalamic location of the intervention effects on fALFF is intriguing considering the white matter microstructure abnormalities in thalamus and cerebellum reported in children and adolescents with NF1 relative to healthy controls (Ferraz-Filho et al., 2012).

Behavioral improvement (false discovery rate adjustment at $\alpha = 0.05$) post-intervention was found for two untrained Cogstate tasks. The increase in Identification task speed after Cogmed program completion might suggest augmentation of domain-general attentional processes. Notably, performance in the Groton Maze Learning task, which highlights spatial working memory demands (Pietrzak et al., 2008), was more accurate after the Cogmed intervention. This finding suggests a degree of generalization of training across spatial working memory processing.

Our preliminary results should be considered in light of limitations beyond small sample size. First, nonspecific intervention benefits cannot be ruled out in the absence of an active control group. Nevertheless, studies have documented Cogmed superiority over non-adaptive contrasts (Astle et al., 2015; Holmes et al., 2009). Indeed, as expected, One-back (i.e., non-adaptive, least challenging working memory task) response times in our sample did not significantly change following Cogmed training. Second, while data quality was adequate, and head micro-motion did not differ pre- and post-training, motion was in the moderate range. Accordingly, we eschewed seed-based analyses, which are particularly susceptible to head motion artifacts (Yan et al., 2013a, 2013b). Third, the finding of focal ReHo effects, while consistent with the ability of TFCE to reliably detect small clusters, should be confirmed in larger samples.

In conclusion, we provide preliminary evidence that regionally specific changes in resting state fMRI measures may capture treatment-related improvements of cognitive dysfunction in NF1. These pilot results should be interpreted with caution pending independent controlled replication.

Supplementary Material

Refer to Web version on PubMed Central for supplementary material.

Acknowledgments

This study was funded by the Children's Tumor Foundation and the Jennifer and Daniel Gilbert Neurofibromatosis Institute at Children's National System.

References

Acosta MT, Gioia GA, Silva AJ. Neurofibromatosis type 1: new insights into neurocognitive issues. Curr Neurol Neurosci Rep. 2006; 6:136–143. [PubMed: 16522267]

Astle DE, Barnes JJ, Baker K, Colclough GL, Woolrich MW. Cognitive training enhances intrinsic brain connectivity in childhood. J Neurosci. 2015; 35:6277–6283. [PubMed: 25904781]

Behzadi Y, Restom K, Liau J, Liu TT. A component based noise correction method (CompCor) for BOLD and perfusion based fMRI. NeuroImage. 2007; 37:90–101. [PubMed: 17560126]

Benjamini Y, Hochberg Y. Controlling the False Discovery Rate: A Practical and Powerful Approach to Multiple Testing. J R Stat Soc Ser B. 1995; 57:289–300.

Cao Q, Zang Y, Sun L, Sui M, Long X, Zou Q, Wang Y. Abnormal neural activity in children with attention deficit hyperactivity disorder: a resting-state functional magnetic resonance imaging study. Neuroreport. 2006; 17:1033–6. [PubMed: 16791098]

Chabernaud C, Mennes M, Kardel PG, Gaillard WD, Kalbfleisch ML, VanMeter JW, Packer RJ, Milham MP, Castellanos FX, Acosta MT. Lovastatin regulates brain spontaneous low-frequency brain activity in Neurofibromatosis type 1. Neurosci Lett. 2012; 515:28–33. [PubMed: 22433254]

Conklin HM, Ogg RJ, Ashford JM, Scoggins MA, Zou P, Clark KN, Martin-Elbahesh K, Hardy KK, Merchant TE, Jeha S, Huang L, Zhang H. Computerized cognitive training for amelioration of cognitive late effects among childhood cancer survivors: A randomized controlled trial. J Clin Oncol. 2015; 33:3894–3902. [PubMed: 26460306]

Constantinidis C, Klingberg T. The neuroscience of working memory capacity and training. Nat Rev Neurosci. 2016; 17:438–449. [PubMed: 27225070]

Cromer JA, Harel BT, Yu K, Valadka JS, Brunwin JW, Crawford CD, Mayes LC, Maruff P. Comparison of cognitive performance on the Cogstate brief battery when taken in-clinic, in-group, and unsupervised. Clin Neuropsychol. 2015; 29:542–558. [PubMed: 26165425]

Eklund A, Nichols TE, Knutsson H. Cluster failure: Why fMRI inferences for spatial extent have inflated false-positive rates. Proc Natl Acad Sci. 2016; 113:7900–7905. [PubMed: 27357684]

Falleti MG, Maruff P, Collie A, Darby DG. Practice effects associated with the repeated assessment of cognitive function using the CogState battery at 10-minute, one week and one month test-retest intervals. J Clin Exp Neuropsychol. 2006; 28:1095–112. [PubMed: 16840238]

Ferraz-Filho JRL, da Rocha AJ, Muniz MP, Souza AS, Goloni-Bertollo EM, Pavarino-Bertelli EC. Diffusion tensor MR imaging in neurofibromatosis type 1: expanding the knowledge of microstructural brain abnormalities. Pediatr Radiol. 2012; 42:449–54. [PubMed: 22033857]

Friston KJ, Williams S, Howard R, Frackowiak RSJ, Turner R. Movement-related effects in fMRI time-series. Magn Reson Med. 1996; 35:346–355. [PubMed: 8699946]

Gioia GA, Isquith PK, Guy SC, Kenworthy L. Behavior rating inventory of executive function. Child Neuropsychol. 2000; 6:235–8. [PubMed: 11419452]

Holmes J, Gathercole SE, Dunning DL. Adaptive training leads to sustained enhancement of poor working memory in children. Dev Sci. 2009; 12:F9–15. [PubMed: 19635074]

Jenkinson M, Bannister P, Brady M, Smith S. Improved optimization for the robust and accurate linear registration and motion correction of brain images. NeuroImage. 2002; 17:825–841. [PubMed: 12377157]

Kelly C, Castellanos FX. Strengthening connections: Functional connectivity and brain plasticity. Neuropsychol Rev. 2014; 24:63–76. [PubMed: 24496903]

Klingberg T, Fernell E, Olesen PJ, Johnson M, Gustafsson P, Dahlström K, Gillberg CG, Forssberg H, Westerberg H. Computerized training of working memory in children with ADHD — a randomized, controlled trial. J Am Acad Child Adolesc Psychiatry. 2005; 44:177–86. [PubMed: 15689731]

Lakens D. Calculating and reporting effect sizes to facilitate cumulative science: a practical primer for t-tests and ANOVAs. Front Psychol. 2013; 4:863. [PubMed: 24324449]

Loitfelder M, Huijbregts SCJ, Veer IM, Swaab HS, Van Buchem MA, Schmidt R, Rombouts SA. Functional connectivity changes and executive and social problems in Neurofibromatosis type 1. Brain Connect. 2015; 5:312–320. [PubMed: 25705926]

Maruff P, Thomas E, Cysique L, Brew B, Collie A, Snyder P, Pietrzak R. Validity of the CogState brief battery: relationship to standardized tests and sensitivity to cognitive impairment in mild traumatic brain injury, schizophrenia, and AIDS dementia complex. Arch Clin Neuropsychol. 2009; 24:165–78. [PubMed: 19395350]

Nee DE, Brown JW, Askren MK, Berman MG, Demiralp E, Krawitz A, Jonides J. A Meta-analysis of executive components of working memory. Cereb Cortex. 2013; 23:264–282. [PubMed: 22314046]

Olesen PJ, Westerberg H, Klingberg T. Increased prefrontal and parietal activity after training of working memory. Nat Neurosci. 2004; 7:75–79. [PubMed: 14699419]

Pietrzak R, Maruff P, Mayes L, Roman S, Sosa J, Snyder P. An examination of the construct validity and factor structure of the Groton Maze Learning Test, a new measure of spatial working memory, learning efficiency, and error monitoring. Arch Clin Neuropsychol. 2008; 23:433–445. [PubMed: 18448309]

Power JD, Mitra A, Laumann TO, Snyder AZ, Schlaggar BL, Petersen SE. Methods to detect, characterize, and remove motion artifact in resting state fMRI. NeuroImage. 2014; 84:320–341. [PubMed: 23994314]

Reuter M, Schmansky NJ, Rosas HD, Fischl B. Within-subject template estimation for unbiased longitudinal image analysis. NeuroImage. 2012; 61:1402–1418. [PubMed: 22430496]

Ribeiro MJ, D'Almeida OC, Ramos F, Saraiva J, Silva ED, Castelo-Branco M. Abnormal late visual responses and alpha oscillations in neurofibromatosis type 1: A link to visual and attention deficits. J Neurodev Disord. 2014; 6:4. [PubMed: 24559228]

Schwetye KE, Gutmann DH. Cognitive and behavioral problems in children with neurofibromatosis type 1: challenges and future directions. Expert Rev Neurother. 2014; 14:1139–1152. [PubMed: 25161109]

Smith SM, Nichols TE. Threshold-free cluster enhancement: addressing problems of smoothing, threshold dependence and localisation in cluster inference. NeuroImage. 2009; 44:83–98. [PubMed: 18501637]

Stevens MC, Gaynor A, Bessette KL, Pearlson GD. A preliminary study of the effects of working memory training on brain function. Brain Imaging Behav. 2016; 10:387–407. [PubMed: 26138580]

Tian L, Ren J, Zang Y. Regional homogeneity of resting state fMRI signals predicts Stop signal task performance. NeuroImage. 2012; 60:539–44. [PubMed: 22178814]

Tomson SN, Schreiner MJ, Narayan M, Rosser T, Enrique N, Silva AJ, Allen GI, Bookheimer SY, Bearden CE. Resting state functional MRI reveals abnormal network connectivity in neurofibromatosis 1. Hum Brain Mapp. 2015; 36:4566–4581. [PubMed: 26304096]

Violante IR, Ribeiro MJ, Cunha G, Bernardino I, Duarte JV, Ramos F, Saraiva J, Silva E, Castelo-Branco M. Abnormal brain activation in Neurofibromatosis type 1: A link between visual processing and the default mode network. PLoS One. 2012; 7:e38785. [PubMed: 22723888]

Wechsler, D. Wechsler Abbreviated Scale of Intelligence (WASI). The Psychological Corporation; San Antonio, TX: 1999.

Wechsler, D. Wechsler Intelligence Scale for Children. 4th. Pearson Corporation; San Antonio, TX: 2004.

Winkler AM, Ridgway GR, Webster MA, Smith SM, Nichols TE. Permutation inference for the general linear model. NeuroImage. 2014; 92:381–97. [PubMed: 24530839]

Yan CG, Cheung B, Kelly C, Colcombe S, Craddock RC, Di Martino A, Li Q, Zuo XN, Castellanos FX, Milham MP. A comprehensive assessment of regional variation in the impact of head micromovements on functional connectomics. NeuroImage. 2013a; 76:183–201. [PubMed: 23499792]

Yan CG, Craddock RC, Zuo XN, Zang YF, Milham MP. Standardizing the intrinsic brain: Towards robust measurement of inter-individual variation in 1000 functional connectomes. NeuroImage. 2013b; 80:246–262. [PubMed: 23631983]

Yang Z, Jutagir DR, Koyama MS, Craddock RC, Yan CG, Shehzad Z, Castellanos FX, Di Martino A, Milham MP. Intrinsic brain indices of verbal working memory capacity in children and adolescents. Dev Cogn Neurosci. 2015; 15:67–82. [PubMed: 26299314]

Zang YF, He Y, Zhu CZ, Cao QJ, Sui MQ, Liang M, Tian LX, Jiang TZ, Wang YF. Altered baseline brain activity in children with ADHD revealed by resting-state functional MRI. Brain Dev. 2007; 29:83–91. [PubMed: 16919409]

Zang Y, Jiang T, Lu Y, He Y, Tian L. Regional homogeneity approach to fMRI data analysis. NeuroImage. 2004; 22:394–400. [PubMed: 15110032]

Zou QH, Zhu CZ, Yang Y, Zuo XN, Long XY, Cao QJ, Wang YF, Zang YF. An improved approach to detection of amplitude of low-frequency fluctuation (ALFF) for resting-state fMRI: Fractional ALFF. J Neurosci Methods. 2008; 172:137–141. [PubMed: 18501969]

Zuo XN, Di Martino A, Kelly C, Shehzad ZE, Gee DG, Klein DF, Castellanos FX, Biswal BB, Milham MP. The oscillating brain: complex and reliable. NeuroImage. 2010a; 49:1432–45. [PubMed: 19782143]

Zuo XN, Kelly C, Di Martino A, Mennes M, Margulies DS, Bangaru S, Grzadzinski R, Evans A, Zang YF, Castellanos FX, Milham MP. Growing together and growing apart: regional and sex differences in the lifespan developmental trajectories of functional homotopy. J Neurosci. 2010b; 30:15034–43. [PubMed: 21068309]

Highlights

- Children with neurofibromatosis type 1 showing working memory deficits participated
- Computerized at-home working memory training intervention was provided for 6–10 weeks
- We obtained pre- and post-treatment resting-state fMRI and cognitive measures
- Two local resting state measures showed regionally specific changes after treatment
- We also observed behavioral improvement on untrained tasks

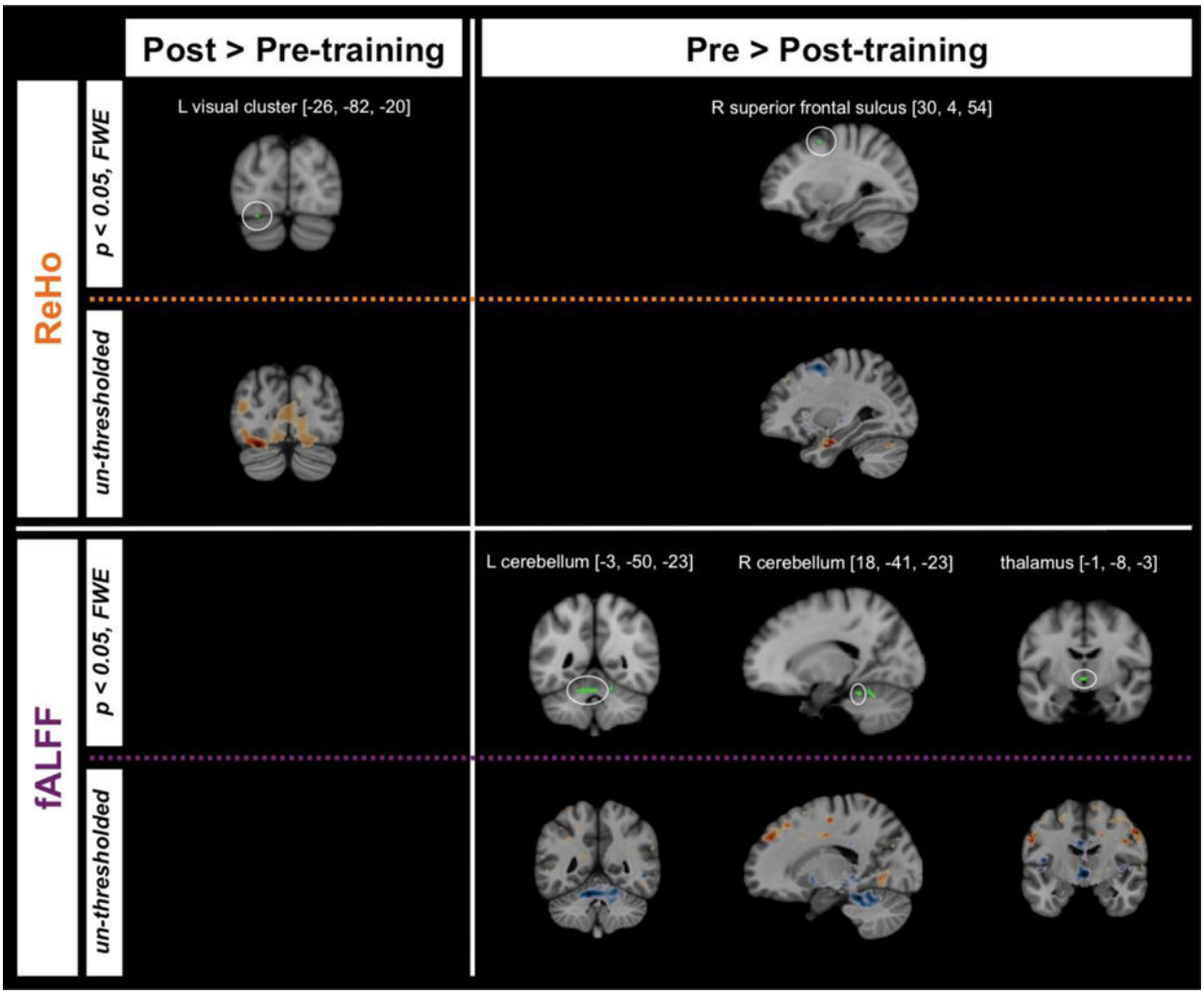

Figure 1.

Clusters showing significant differences *(p* < 0.05, family-wise error corrected) in brain resting state measures pre-Cogmed relative to post-Cogmed training overlaid on the MNI152 T1 template. Corresponding un-thresholded maps for each cluster for each contrast and measure are provided directly underneath each significant effect. Un-thresholded whole-brain maps for all four measures are freely viewable at http://neurovault.org/collections/ZLEIBWYV).

fALFF = fractional amplitude of low frequency fluctuations; L = left; MNI = Montreal Neurological Institute; TFCE = threshold-free cluster enhancement; ReHo = regional homogeneity; R = right.

Table 1

Participant (*n* = 16) demographic characteristics and cognitive abilities assessed prior to training

	Mean ± SD	Range
Boys, *n* (%)	9 (56%)	
Age (years)	11.1 ± 2.3	8–15
Wechsler Intelligence Scale for Children-IV (standard scores)		
Full Scale IQ	93.2 ± 8.1	79–106
Working Memory Index	89.9 ± 11.6	71–113
Behavior Rating Inventory of Executive Function (T scores)		
Working Memory	66.3 ± 9.0	51–79
Metacognitive Index	66.3 ± 6.9	51–74
Behavioral Regulation Index	61.6 ± 12.4	41–84

SD = standard deviation; IQ = intelligence quotient

Table 2

Age-normed behavioral performance on Cogstate tasks before and after Cogmed training along with paired *t*-test contrasts assessing improvement after training.

	pre-Cogmed (M ± SE)	post-Cogmed (M ± SE)	t_{15}	*p*	*fdr-adjusted p*	Hedges' g_{av} corrected effect size
Identification speed	96.2 ± 3.0	106.3 ± 3.0	−4.77	0.00025	0.0012	0.82
Groton Maze Learning errors	89.2 ± 4.9	95.6 ± 4.8	−3.01	0.0087	0.0219	0.32
Detection speed	101.0 ± 1.9	105.8 ± 2.2	−2.34	0.0334	0.0557	0.57
One-back speed	102.0 ± 2.8	103.1 ± 3.9	−0.38	0.7128	0.7128	0.08
One Card Learning accuracy	91.0 ± 2.4	94.6 ± 2.5	−1.25	0.2300	0.2875	0.35

Note: Higher scores indicate better performance.

fdr, false discovery rate; M, mean; SE, standard error of the mean

Table 3

Significant differences in brain resting-state measures per nonparametric permutation analysis

	Cluster				
	Voxels	Center of gravity (MNI)			Major structures associated with cluster
		x	y	z	
Contrast					
fALFF pre > post-training					
	200	−2.5	−49.6	−23.0	L cerebellum I-IV, L cerebellum V
	27	18.3	−41.1	−23.3	R cerebellum V, R cerebellum I-IV
	26	−0.8	−8.1	−3.2	L thalamus, R thalamus
ReHo pre > post-training					
	3	30.0	4.7	55.3	R superior frontal sulcus (R middle frontal gyrus)
ReHo post > pre-training					
	3	−27.3	−81.3	−20.0	L occipital fusiform gyrus

Probabilistic anatomical labels were obtained using *fsl*'s function *atlas query* with atlas inputs *Harvard-Oxford Cortical Structural, Harvard-Oxford Subcortical Structural* or *Cerebellar Atlas in MNI152 space after normalization with FNIRT*. Locations of voxels with peak statistic values within each cluster are depicted in Figure 1.

fALFF = fractional amplitude of low frequency fluctuations; L = left; MNI = Montreal Neurological Institute; ReHo = regional homogeneity; R = right